**TEKNISKA HÖGSKOLAN I LUND**
MATEMATISKA INSTITUTIONEN

LUTFD2 - TFMA -- 92 - 7002.

# Principles of Doppler Tomography

## Peter Juhlin

# Principles of Doppler Tomography

Peter Juhlin

Department of Mathematics

Lund Institute of Technology

P.O. Box 118

S-221 00 Lund

Sweden

August 17, 1992

### Abstract

This paper shows how the Radon Transform can be used to determine vector fields. A scheme to determine the velocity field of a moving fluid by measurements with a continuous Doppler signal is suggested. When the flow is confined to a bounded domain, as is the case in most applications, it can be uniquely decomposed into one gradiental and one rotational part. The former vanishes if the fluid is incompressible and source-free, and the latter can be completely reconstructed by the methods proposed in this paper if the domain is simply connected.

Special attention is paid to laminar flow in a long cylindrical vessel with circular cross-section. Under such conditions the flow profile becomes parabolic, which makes the vessel recognizable as a typical "N-shaped" pattern in an image describing the rotation of the velocity field. The vessel yields the same Doppler tomographic pattern, no matter how it is sectioned. The ideas presented should be applicable also when studying the flow in blood vessels, even if the flow profile in these is not quite parabolic. The discrepancies only make the "N-shape" somewhat distorted.

# The scalar Radon Transform

The Radon and related transforms are currently in wide use in the fields of applied mathematics. In particular, during the last decade medical imaging techniques have turned more and more towards tomography. X-ray Computed Tomography (CT), Emission CT, Ultrasound CT and Nuclear Magnetic Resonance Imaging are the dominant areas. The enormous increase in computer power available at a relatively low cost is probably the single most important factor behind this development. Advances in electronics and improved computer algorithms have also contributed. However, the underlying mathematics is much the same as before. Typically, the issue is to measure how a tissue scatters or absorbs the energy in an applied test beam. The equation governing this process can often be written as

$$ I \;=\; I_0 \exp\left(-\int_L \mu(\mathbf{r})\,dl\right), $$

where $I$ is the intensity of the test beam and $L$ is the path that the beam takes. The object is to determine how the linear attenuation coefficient, $\mu(x)$, varies in space.

Consider a transverse section of a three dimensional body of finite extent. Introduce an orthogonal coordinate system such that the section lies in the $xy$ plane. Each straight line in this plane is uniquely determined by the pair $(s,\theta)$, defined in Figure 1 below. Note that $-\infty < s < \infty$ and $0 \le \theta < \pi$. Let $\boldsymbol{\omega}$ denote the unit vector $\boldsymbol{\omega} = (\cos\theta, \sin\theta, 0)$. Then $\boldsymbol{\omega}$ and $\theta$ are interchangeable, and the line $L$ can be written in the form

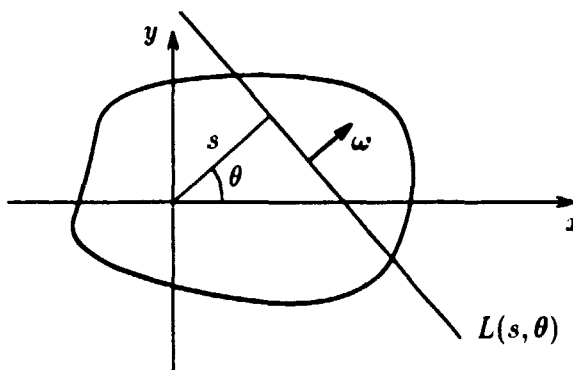$$ L(s,\theta) \;=\; \{\mathbf{r}: \mathbf{r}\cdot\hat{\mathbf{e}}_z = 0,\; \mathbf{r}\cdot\boldsymbol{\omega} = s\}. $$



Figure 1: Definition of the parameters for the Radon transform.

Let us now confine ourselves to the plane $z = 0$, and introduce the function $\check{\mu}$ as

$$ \check{\mu}(s,\theta) \;=\; -\log\left(\frac{I}{I_0}\right) \;=\; \int_{\substack{\mathbf{r}\cdot\boldsymbol{\omega}=s \\ z=0}} \mu(\mathbf{r})\,dl. $$

2

Then $\check{\mu}$ is the two dimensional Radon transform (or X-ray transform) of $\mu$ which we also write $\check{\mu}(s,\theta) = \mathcal{R}\mu$.

Measuring how a test beam is attenuated along a straight line, $L(s,\theta)$, one can evaluate $\check{\mu}(s,\theta)$, and as $s$ and $\theta$ vary to generate any line in the $xy$ plane, the function $\check{\mu}(s,\theta)$ can be obtained for the entire $s\theta$ plane. With the aid of the inverse Radon transform, $\mu = \mathcal{R}^{-1}\check{\mu}$, it is then possible to calculate the linear attenuation coefficient, $\mu(x,y)$, at any point in the $xy$ plane. For further background on the scalar Radon transform, the reader is referred to [3] and [4].

## Moving Fluids and Doppler Shift

If the domain under consideration contains a moving fluid, then the Doppler shift can be used to measure the velocity of this motion. Disregarding relativistic effects, the Doppler shift, $\Delta\omega$, in an emitted signal with angular frequency $\omega$ is described by the equation

$$\Delta\omega = \frac{2cu\omega}{c^2 - u^2},$$

where $c$ is the velocity of sound in the medium inside the body and $u$ is the velocity with which the object inducing the Doppler shift approaches the sound source. Under conditions realistic in medicine, $u \ll c$, so to a good approximation

$$\Delta\omega = \frac{2u\omega}{c},$$

i.e., $\Delta\omega$ is proportional to the velocity at which the reflecting object approaches the Doppler probe. If the intention is to evaluate the velocity of the fluid at a certain spot, one can transmit a well focused beam of fairly short duration. When this test beam runs into an obstacle, some of its intensity is reflected and the rest is transmitted through the obstacle. The latter part will be further divided into reflected and transmitted parts when it runs into new obstacles, and so forth. Considering the time it takes for a certain part of the signal to return to the transmitter/receiver, it is possible to calculate how far it went before it was reflected. Hence, measuring how the Doppler shift from one short pulse varies with time, it is possible to tell the velocity of the various objects "lit up" by the test beam. To be able to measure the velocity of a fluid this way, it is of course necessary that the fluid contains some particles that reflect the test beam. In the human body, the fluid is typically blood that contains numerous red blood cells which can generate the Doppler shift wanted.

## The Radon Transform and Vector Fields

The method described above with a "pulsed Doppler" seems to make tomography superfluous. However, for technical reasons it is often more convenient to transmit with a "continuous Doppler", and then one loses the information of where (at what distance from the probe) a certain part of the Doppler shift is generated. Instead one receives a continuous signal that consists of a Doppler broadening of the transmitted

3

angular frequency. From this Doppler broadened signal it is possible to calculate the mean value of the velocity component parallel to the test beam, the averaging being made over the "tube" lit up by the test beam. Hence, after some signal processing, one gets an integral over the test beam, similar to the one for $\bar{\mu}$ above, but now with $\hat{\mathbf{e}}_z \cdot \boldsymbol{\omega} \times \mathbf{f}(\mathbf{r})$. i.e., the velocity component parallel to the test beam, as integrand. Here $\mathbf{f}(\mathbf{r})$ denotes the velocity field. Let $\mathcal{D}\mathbf{f}$ denote this processed measurement of the $\mathcal{D}$oppler shift, i.e.,

$$\mathcal{D}\mathbf{f}(s,\boldsymbol{\omega}) = \int_{\substack{\mathbf{r}\cdot\boldsymbol{\omega}=s \\ z=0}} \hat{\mathbf{e}}_z \cdot \boldsymbol{\omega} \times \mathbf{f}(\mathbf{r})\, dl. \tag{1}$$

The issue is now to regain $\mathbf{f}$ from $\mathcal{D}\mathbf{f}$ through a process similar to the inverse two dimensional Radon transform. The integrand in equation (1) is a scalar, and hence it might seem as if the inverse Radon transform is applicable in a straightforward manner. However, the integrand depends not only on $\mathbf{r}$, but also on $\boldsymbol{\omega}$. The idea to circumvent this difficulty is to use Stokes' theorem. Consider two parallel test beams close to each other. In mathematical terms, consider the two line integrals $\mathcal{D}\mathbf{f}(s,\boldsymbol{\omega})$ and $\mathcal{D}\mathbf{f}(s+\varepsilon,\boldsymbol{\omega})$ in Figure 2. Since the body containing the fluid is of finite
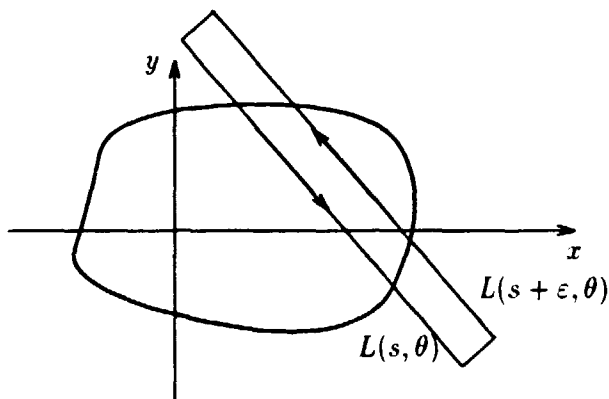


Figure 2: Doppler measurements along two adjecent lines. The path is closed outside the body without changing the value of the total integral.

extent, the lines $L(s,\theta)$ and $L(s+\varepsilon,\theta)$ can be cut off anywhere outside the body without changing the values of the integrals. Furthermore one can, without adding anything to the integral, close the integration path anywhere outside the body with two short lines parallel to $\boldsymbol{\omega}$ (as in Figure 2). Let $\Omega_\varepsilon$ denote the planar region thus enclosed by the rectangular path $\partial\Omega_\varepsilon$. According to Stokes' theorem,

$$\int_{\partial\Omega_\varepsilon} \mathbf{f}(\mathbf{r}) \cdot d\mathbf{r} = \int_{\Omega_\varepsilon} \nabla \times \mathbf{f}(\mathbf{r}) \cdot d\mathbf{S},$$

and hence,

$$\mathcal{D}\mathbf{f}(s+\varepsilon,\boldsymbol{\omega}) - \mathcal{D}\mathbf{f}(s,\boldsymbol{\omega}) = \int_{\substack{\mathbf{r}\cdot\boldsymbol{\omega}=s+\varepsilon \\ z=0}} \hat{\mathbf{e}}_z \cdot \boldsymbol{\omega} \times \mathbf{f}(\mathbf{r})\, dl - \int_{\substack{\mathbf{r}\cdot\boldsymbol{\omega}=s \\ z=0}} \hat{\mathbf{e}}_z \cdot \boldsymbol{\omega} \times \mathbf{f}(\mathbf{r})\, dl$$

4

$$= \int_{\partial\Omega_\epsilon} \mathbf{f}(\mathbf{r}) \cdot d\mathbf{r}$$

$$= \int_{\Omega_\epsilon} \hat{\mathbf{e}}_z \cdot \nabla \times \mathbf{f}(\mathbf{r}) \, dS.$$

Dividing all members by $\epsilon$ and letting $\epsilon \to 0$, one gets

$$\frac{\partial}{\partial s}\mathcal{D}\mathbf{f}(s,\omega) = \int_{\substack{\mathbf{r}\cdot\omega=s \\ z=0}} \hat{\mathbf{e}}_z \cdot \nabla \times \mathbf{f}(\mathbf{r}) \, dl, \tag{2}$$

at least if $\mathbf{f} \in C^1$. Referring to distribution theory, the same can be shown to hold also for less regular velocity fields, $\mathbf{f}$. One only needs $\mathbf{f}$ to be regular enough for the $\mathcal{D}\mathbf{f}$-integrals to be well-defined distributions. Here the right hand side is a scalar planar Radon transform, and hence one can regain $\hat{\mathbf{e}}_z \cdot \nabla \times \mathbf{f}(\mathbf{r})$ for all $\mathbf{r}$ lying in the plane $z = 0$,

$$\hat{\mathbf{e}}_z \cdot \nabla \times \mathbf{f}(x,y,0) = \mathcal{R}^{-1}\left(\frac{\partial}{\partial s}\mathcal{D}\mathbf{f}(s,\omega)\right).$$

Similarly can be done for other values of $z$, yielding $\hat{\mathbf{e}}_z \cdot \nabla \times \mathbf{f}(\mathbf{r})$ for all $\mathbf{r}$. Rotating the body ninety degrees, one can of course also determine the $x$-component, $\hat{\mathbf{e}}_x \cdot \nabla \times \mathbf{f}(\mathbf{r})$, and finally the $y$-component. Thus, the rotation of the velocity field can be completely recovered through the proposed tomographic Doppler procedure.

# Decomposing and Reconstructing a Vector Field

Having determined the rotation of the velocity field, the question arises how this can be used to regain the velocity field itself. One can easily construct two different fields which have the same rotation, so obviously knowledge of the rotation of a field is not sufficient to determine the complete field. Instead one is led to study an orthogonal decomposition of the field into one rotational and one gradiental part. Such decompositions date back to Helmholtz and the middle of the nineteenth century. Depending on the prescribed boundary conditions and the regularity imposed on the field, various forms of the decomposition theorem have been established. The following version is adapted to a fluid flow confined to a bounded domain, and can be found on page 51 in [2].

**Theorem 1 (Decomposition of a Vector Field)** *Let $\Omega$ be an open bounded domain in $\mathbf{R}^3$ with a piecewise $C^1$-boundary, $\partial\Omega$, let $\mathbf{n}$ denote the outwards directed unit normal to $\partial\Omega$, and let $\mathbf{f}$ be a vector field, such that $\mathbf{f} \in L^2(\Omega)$ and $\mathbf{n}\cdot\mathbf{f} \in L^2(\partial\Omega)$. Then $\mathbf{f}$ can be decomposed in a solenoidal part, $\mathbf{u}$, and an irrotational part, $\nabla p$,*

$$\mathbf{f} = \mathbf{u} + \nabla p.$$

*If it is required that $\mathbf{u} \cdot \mathbf{n} = 0$ in $L^2(\partial\Omega)$, then the decomposition becomes unique, and both parts, $\mathbf{u}$ and $\nabla p$, belong to $L^2(\Omega)$.*

The decomposition described means that **u** contains all the rotation of **f**, whereas the divergence of **f** is entirely in $\nabla p$, and so is the normal component across the boundary.

Closely connected to the described decomposition of the field into orthogonal components is the reconstruction of a field from knowledge of its rotation and divergence within the domain and its normal component across the boundary. The following theorem is in a sense quite basic in vector analysis, and again an analogue for unbounded regions, with the boundary condition replaced by vanishing conditions at infinity, was shown already by Helmholtz. However, the version presented below seems hard to find in the literature.

**Theorem 2 (Reconstruction of a Vector Field)** *Let $\Omega$ be a simply connected open bounded domain in* $\mathbf{R}^3$ *with a piecewise* $C^1$-*boundary, $\partial\Omega$, let* $\mathbf{q}, \varphi \in \mathcal{E}'(\Omega) + L^2(\Omega)$ *and* $\psi \in L^2(\partial\Omega)$. *Then the following boundary value problem,*

$$\begin{aligned} \nabla \times \mathbf{f} &= \mathbf{q} \quad in \ \Omega \\ \nabla \cdot \mathbf{f} &= \varphi \quad in \ \Omega \\ \mathbf{n} \cdot \mathbf{f} &= \psi \quad on \ \partial\Omega, \end{aligned}$$

*has a unique solution in* $\mathcal{E}'(\Omega) + L^2(\Omega)$ *if*

$$\int_\Omega \varphi \, dV = \int_{\partial\Omega} \psi \, dS.$$

*Otherwise no solution exists.*

*Proof:*
We start by constructing a vector field **g** in $\mathbf{R}^3$ that satisfies the equations

$$\nabla \times \mathbf{g} = \mathbf{q} \quad \text{in } \mathbf{R}^3 \tag{3}$$
$$\nabla \cdot \mathbf{g} = \varphi \quad \text{in } \mathbf{R}^3, \tag{4}$$

where **q** and $\varphi$ are compactly supported in $\overline{\Omega}$. If such a **g** exists, it follows from the vector identity

$$\Delta \mathbf{g} = \nabla(\nabla \cdot \mathbf{g}) - \nabla \times (\nabla \times \mathbf{g})$$

and the concept of a fundamental solution that

$$\begin{aligned} \mathbf{g} &= E * \{\nabla(\nabla \cdot \mathbf{g}) - \nabla \times (\nabla \times \mathbf{g})\} \\ &= E * \{\nabla\varphi - \nabla \times \mathbf{q}\}, \end{aligned}$$

where $E(\mathbf{r}) = -\frac{1}{4\pi|\mathbf{r}|}$. Since **q** and $\varphi$ have compact support, the convolutions are well-defined, and it is easily verified that this **g** satisfies equations (3) and (4) and that $\mathbf{g} \in H^1(\Omega)$. However, the vector field, **g**, does not satisfy the boundary condition. For that reason we consider an additional boundary value problem,

$$\begin{aligned} \nabla \times \mathbf{h} &= 0 \quad \text{in } \Omega \\ \nabla \cdot \mathbf{h} &= 0 \quad \text{in } \Omega \\ \mathbf{n} \cdot \mathbf{h} &= \tilde{\psi} \quad \text{on } \partial\Omega, \end{aligned}$$

where $\dot{v} = v - \mathbf{n} \cdot \mathbf{g}$. Through superposition, one realizes that $\mathbf{f} = \mathbf{g} + \mathbf{h}$ solves the original boundary value problem, and that it only remains to determine $\mathbf{h}$.

Obviously, $\Delta \mathbf{h} = 0$ in $\Omega$, and hence $\mathbf{h} \in C^\infty(\Omega)$. Since $\nabla \times \mathbf{h} = 0$ on the simply connected domain, $\Omega$, classical vector analysis then guarantees the existence of a scalar potential, $\phi \in C^\infty(\Omega)$, such that $\mathbf{h} = \nabla \phi$ in $\Omega$. Inserting this in the other two equations for $\mathbf{h}$ yields

$$\begin{aligned} \nabla \cdot (\nabla \phi) &= 0 \\ \mathbf{n} \cdot \nabla \phi &= \tilde{\psi}, \end{aligned}$$

i.e.,

$$\begin{aligned} \Delta \phi &= 0 \\ \frac{\partial \phi}{\partial n} &= \tilde{\psi}. \end{aligned}$$

Provided that $\int \tilde{\psi} \, dS = 0$, this Neumann boundary value problem determines a solution, $\phi \in H^{3/2}(\Omega)$, unique up to an additive constant, which means that $\mathbf{h}$ is uniquely determined, and $\mathbf{h} \in H^{1/2}(\Omega)$. The condition on $\tilde{\psi}$ may be restated as

$$\begin{aligned} \int_\Omega \nabla \cdot \mathbf{f} \, dV &= \int_{\partial\Omega} \mathbf{f} \cdot \mathbf{n} \, dS \\ \int_\Omega \varphi \, dV &= \int_{\partial\Omega} \psi \, dS. \end{aligned}$$

$\square$

*Remark:*
The proof presented above provides a constructive method to regain $\mathbf{f}$.

It should also be noted that the regularity conditions on the various right hand members in the theorem are not the optimal ones. For instance, the theorem does not cover the simple case of an ideal fluid moving with a constant velocity in a straight circular tube inside a cubic body, entering on one side and leaving at the opposite, the tube being orthogonal to the sides of the cube. For such a velocity field, the rotation, $\mathbf{q} := \nabla \times \mathbf{f}$, gets too singular to belong to $L^2$ near the boundary. It is however easy to adopt the above proof to the case with fields $\varphi, \mathbf{q} \in \mathcal{D}'(\Omega)$ such that the singularities of these fields are transversal to $\partial\Omega$.

## The rotational part

Now, let $\Omega$ denote the body containing the moving fluid, and let $\mathbf{f}$ denote the velocity field of the fluid. Since no fluid leaves the body, $\mathbf{n} \cdot \mathbf{f} = 0$ on $\partial\Omega$. The Doppler tomography described yields $\nabla \times \mathbf{f}$, and decomposing the field according to Theorem 1, it actually gives $\nabla \times \mathbf{u}$, since $\nabla \times \nabla p = 0$. By assumption the $\mathbf{u}$ field is solenoidal, i.e., $\nabla \cdot \mathbf{u} = 0$, so both the rotation and the divergence of $\mathbf{u}$ are known. Furthermore, the constraint $\mathbf{n} \cdot \mathbf{u} = 0$ has been imposed on $\mathbf{u}$, so relying on Theorem 2 one can say that the tomographic procedure in essence yields $\mathbf{u}$, the rotational part of $\mathbf{f}$.

### The gradiental part

As is shown below, the gradiental part of **f** does not influence the Doppler measurements at all. However, under the assumption of incompressibility, $\nabla p$ must vanish.

Decomposing as above and making use of the linearity of the $\mathcal{D}$-operator, let us investigate $\mathcal{D}(\nabla p)$ while measuring along an arbitrary line, $L$, that intersects $\partial\Omega$ in the points $l_0$ and $l_1$.

$$
\begin{aligned}
\mathcal{D}(\nabla p) &= \int_L \hat{\mathbf{e}}_z \cdot \boldsymbol{\omega} \times \nabla p \, dl \\
&= \int_L \frac{\partial p}{\partial l} \, dl \\
&= p(l_1) - p(l_0),
\end{aligned}
$$

since the integrand is the component of $\nabla p$ along $L$. Measuring along various lines, one can obviously determine $p$ at the boundary up to an additive constant. But that is all the information obtainable from Doppler measurements.

Since both $\mathbf{n} \cdot \mathbf{f}$ and $\mathbf{n} \cdot \mathbf{u}$ vanish on the boundary, the same must hold for $\mathbf{n} \cdot \nabla p = \frac{\partial}{\partial n} p$. Hence, knowledge of $\nabla \cdot \mathbf{f} = \nabla^2 p$ in $\Omega$ is exactly what we require in order to determine $p$ (up to an additive constant) in the interior of $\Omega$. If the flow is source-free and incompressible, which is quite a reasonable assumption when fluids are concerned, then $\nabla \cdot \mathbf{f} = 0$, and hence $\nabla p = 0$. Thus, for incompressible fluids the velocity field, $\mathbf{f}$, can be exactly regained by the Doppler tomography suggested ·in this paper.

At the same time as it is unfortunate that the gradiental part is unobtainable from Doppler measurements, it is pleasant that it at least does not disturb $\frac{\partial}{\partial s}\mathcal{D}\mathbf{f}$.

*Remark:*
We have seen already in equation (2) that a gradiental part makes no contribution to $\frac{\partial}{\partial s}\mathcal{D}\mathbf{f}$. Referring to this equation is a bit unsatisfactory, though, since the calculations behind it include a limiting process where $\varepsilon \to 0$, and when it comes to numerics, such operations might be quite sensitive to discretization errors.

Instead we note that calculating $\frac{\partial}{\partial s}\mathcal{D}\mathbf{f}$ means measuring the integral

$$
\frac{\partial}{\partial s}\mathcal{D}\mathbf{f} = \oint_{\partial\Omega_\epsilon} \mathbf{f}(\mathbf{r}) \cdot d\mathbf{r}
$$

along a closed rectangular path, and for a pure gradient, $\mathbf{f} := \nabla p$, it holds that

$$
\oint \{\nabla p(\mathbf{r})\} \cdot d\mathbf{r} = 0
$$

along any closed path, i.e., the vanishing does not depend critically on any limiting process.

**Doppler Tomography in summary**

To summarize, the scheme for analyzing the velocity field of an *incompressible* fluid with Doppler tomography is as follows:

- Measure the parallel component of the mean velocity along each line in the plane $z = 0$, and denote it $\mathcal{D}\mathbf{f}$.

- Differentiate $\mathcal{D}\mathbf{f} = \mathcal{D}\mathbf{f}(s, \boldsymbol{\omega})$ with respect to $s$ to get
  $\frac{\partial}{\partial s}\mathcal{D}\mathbf{f} = \mathcal{R}(\hat{\mathbf{e}}_z \cdot \nabla \times \mathbf{f}(x, y, 0))$.

- Apply the inverse planar Radon transform to regain $\hat{\mathbf{e}}_z \cdot \nabla \times \mathbf{f}(x, y, 0)$.

- Repeat the whole procedure for all other values of $z$.

- Rotate the body so that $\hat{\mathbf{e}}_x \cdot \nabla \times \mathbf{f}$ and $\hat{\mathbf{e}}_y \cdot \nabla \times \mathbf{f}$ can be obtained similarly.

- The physically reasonable boundary condition is $\mathbf{n} \cdot \mathbf{f} = 0$, and since the fluid is incompressible, $\nabla \cdot \mathbf{f} = 0$. According to Theorem 2, it is thus possible to reconstruct $\mathbf{f}$ itself from the full knowledge of $\nabla \times \mathbf{f}$.

*Remark:*
Theoretically, in the procedure presented above, the Doppler measurements to determine the $\hat{\mathbf{e}}_y$-component of the rotation, after the $\hat{\mathbf{e}}_z$- and $\hat{\mathbf{e}}_z$-components have already been regained, are actually superfluous, since the $\hat{\mathbf{e}}_y$-component can be calculated from $\hat{\mathbf{e}}_z \cdot \nabla \times \mathbf{f}$ and $\hat{\mathbf{e}}_x \cdot \nabla \times \mathbf{f}$ in a straightforward manner. We have namely $\nabla \cdot \nabla \times \mathbf{f} = 0$, so

$$
\begin{aligned}
\hat{\mathbf{e}}_y \cdot \nabla \times \mathbf{f}(x, y, z) &= \int_{-\infty}^{y} \frac{\partial}{\partial \eta} \hat{\mathbf{e}}_y \cdot \nabla \times \mathbf{f}(x, \eta, z) \, d\eta \\
&= -\int_{-\infty}^{y} \frac{\partial}{\partial x} \hat{\mathbf{e}}_x \cdot \nabla \times \mathbf{f}(x, \eta, z) + \frac{\partial}{\partial z} \hat{\mathbf{e}}_z \cdot \nabla \times \mathbf{f}(x, \eta, z) \, d\eta.
\end{aligned}
$$

A vector field, $\mathbf{f}$, has three degrees of freedom, and one of these is controlled by the divergence, while the other two are connected to the rotation. However, determining the third component from the other two would be quite an unstable method.

## Practical aspects

The procedure outlined above describes how one *in theory* can reconstruct the flow of an incompressible fluid from measurements with a continuous Doppler signal. The only restriction is that the fluid must be contained in a bounded and simply connected domain. There are major practical difficulties, though. The Doppler beam should have an infinitely small diameter, so the body must be tomographed in infinitely many slices to determine the rotation of the flow. Furthermore, through the convolution with $-1/4\pi r$, the rotation in one point influences the reconstructed flow also in every other point of the body. Hence, one needs to determine the rotation in the whole body before the flow can be calculated in any part of it.

In practice one has to assume certain smoothness properties of the flow, in order to make a finite diameter of the Doppler beam acceptable. One also has to discretize the body to implement the tomographic procedure on a computer. The rotation can then be determined with a fair degree of accuracy. However, when we want to reconstruct the flow, $\mathbf{f}$, from its rotation after having imposed the physical conditions, $\nabla \cdot \mathbf{f} = 0$ and $\mathbf{n} \cdot \mathbf{f} = 0$, the result will probably be rather distorted. This is expected, since the reconstruction algorithm presented in the proof of Theorem 2 contains a lot of manipulations with the calculated slightly inaccurate rotation data. Furthermore, the calculations will be rather heavy. Even if the inversion part of the reconstruction (the calculation of the rotation) can be performed one slice at a time. one has to take the whole three dimensional body into consideration in the forward problem when determining the ctual velocity field.

To summarize, the above procedure leaves a great deal to be desired. Fortunately however, there are short-cuts when it comes to studying blood flow in arteries and veins.

10

# Application to Blood Flows

The flow of a linearly viscous fluid is governed by the Navier-Stokes' equation together with appropriate boundary conditions.

$$\rho \frac{D\mathbf{u}}{Dt} = -\nabla p + (\lambda + \mu)\nabla(\nabla \cdot \mathbf{u}) + \mu\Delta\mathbf{u} + \rho\mathbf{b} \quad \text{in } \Omega$$
$$\mathbf{u} = 0 \quad \text{on } \partial\Omega.$$

The notation is here in accordance with chapter 1.3 in [2], and $\mathbf{u}$ denotes the velocity field, $\mathbf{b}$ the body force per unit mass, $p$ the pressure, $\rho$ the density of the fluid, $\mu, \lambda$ the coefficients of viscosity, and $\frac{D}{Dt} = \frac{\partial}{\partial t} + \mathbf{u} \cdot \nabla$ the material time-derivative. This boundary value problem is very hard to solve in the general case, and for that reason simplifying assumptions are usually imposed. In the special case of blood flow, it is a good approximation to regard the fluid to be homogeneous, linearly viscous, and incompressible. The gravitational body force is often ignored, and a further approximation is to neglect the $\frac{D\mathbf{u}}{Dt}$-term. The motivation for the latter when studying Navier-Stokes' equation is usually that the fluid is in a slow steady-state motion. Such a motivation would not be quite appropriate for the pulsatile blood flow in large arteries, but let us neglect the material time-derivative anyhow, just to make the calculations feasible. Together, these simplifications reduce Navier-Stokes' equation to

$$\begin{cases} \Delta\mathbf{u} &= \frac{1}{\mu}\nabla p \\ \nabla \cdot \mathbf{u} &= 0. \end{cases}$$

Finally, considering the blood vessels to be long cylinders with circular cross section, and taking the boundary conditions into consideration, the fluid velocity gets a parabolic flow profile. In cylindrical coordinates,

$$\mathbf{u} = \frac{1}{2\mu}\frac{\partial p}{\partial z}(\rho^2 - R^2)\,\hat{\mathbf{e}}_r. \tag{5}$$

where $\frac{\partial p}{\partial z}$ is a negative constant, $R$ the radius of the vessel, and $\rho$ the distance from the axis of the vessel, $\rho \leq R$. The rotation of such a velocity field has a linear profile that is "N-shaped" in a plane tomographic section. The profile has the same shape, no matter how the vessel is sectioned, as long as the flow is not exactly transversal to the section. This means that to detect such a blood flow, it suffices to make one tomographic section. It is not necessary to have the whole body tomographed. Furthermore, this profile lends itself to "pattern recognition", which means that the vessel can be detected also under suboptimal conditions for the data acquisition.

Blood flowing in blood vessels does not behave exactly as predicted by (5), but empirically the parabolic flow profile has proved to be a fairly good approximation. When the blood flow is accelerated, the profile becomes more like a "plug", cf. Figure 3. In mathematical terms one can approximate it as

$$\mathbf{u} = C\left(1 - \left(\frac{\rho}{R}\right)^{\alpha}\right)\hat{\mathbf{e}}_r.$$

where $C = C(\mu, \frac{\partial p}{\partial z}, R)$ is a positive function and the exponent $\alpha \geq 2$ increases when the blood flow is accelerated. The rotation field is still "N-shaped" with an easily
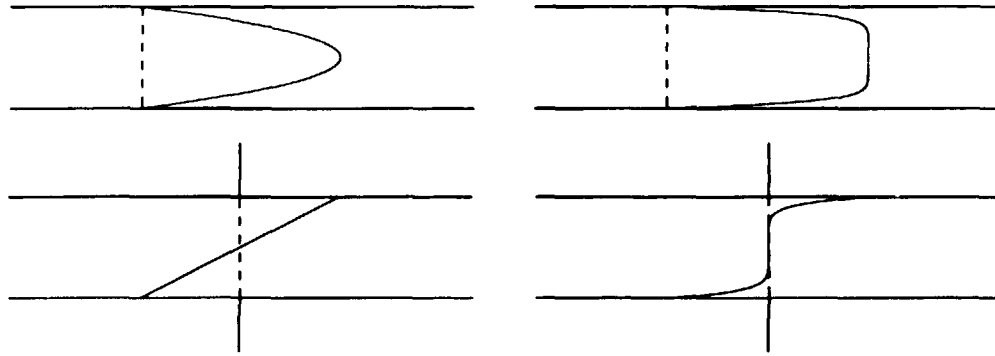
Figure 3: Blood flow in a long cylinder with circular cross-section. The blood flows along the $x$-axis, and the section is paralell to the $xy$-plane. To the left is a parabolic flow with the corresponding "N-shaped" $z$-component of the rotation field. To the right is a "plug flow" and the deformed "N" belonging to that flow.

detectable pattern, although the "N" gets somewhat distorted. However, if the main arteries are narrowed for some reason, the flow in them might become turbulent. The rotation field then gets stirred up, and there will no longer be any recognizable "N-shape".

If the fluid is confined to certain vessels, and if the flow in such a vessel is parallel to the vessel, then one can calculate the velocity just by integrating the rotation field. This simplifies the reconstruction of the velocity field a great deal, since there will be no need to take the whole three dimensional body into consideration.

A practical restriction when using Doppler tomography to determine a flow is that the tomographic procedure takes some time to carry out, so the flow should rather be stationary. In medicine, when measuring blood flow in vessels, the flow is usually not stationary but pulsatile. However, Doppler tomography might still be applicable. The idea is just to use the ECG signal to trigger the test beam, so that all tomographic data are collected from the same part of the heart cycle. This is called "gating".

To speed up the data acquisition, it should be possible to use a number of probes simultaneously, each transmitting with its own frequency. The Doppler broadening is rather narrow, so over-hearing is no problem.

# Simulation studies

The Doppler tomography suggested above to regain the rotation of a velocity field has been tried out in computer simulations. In a $32 \times 32$ mesh, the various grid points have been assigned velocities corresponding to a plane parabolic flow in a cylindrical vessel that has been sectioned longitudinally. The results of the "Doppler measurements" along straight lines have been calculated, and the $s$-derivative has been evaluated through finite differences. With $\frac{\partial}{\partial s}\mathcal{D}\mathbf{f}$ as input data, an inversion of the Radon transform has been carried out to regain $\hat{\mathbf{e}}_z \cdot \nabla \times \mathbf{f}$. For this, a modified version of the discrete Radon transform according to Beylkin [1] has been implemented. Beylkin's scheme was primarily designed for geophysical applications, which means long narrow bore holes, whereas the dimensions of the human body are more like those of a sphere or a cube. As a practical consequence, when the scheme is applied to Doppler tomography, certain directions of the flow are much easier to detect than others, since Beylkin's method confines the "Doppler probe" to one of the "long sides" of the body under investigation. Hence, flow parallel to the "long sides" generates a rather low signal to noise ratio, whereas flow orthogonal to the "long sides" gives very accurate signals.

Below are two examples of parabolic flow. The input data for the simulations are the $x$- and $y$-components of the planar flow. Each mesh point is assigned a velocity vector. In the first example, Figure 4, the flow is parallel to one of the sides of the quadratic body, and the reconstruction of the flow is excellent. The "probe" is confined to the side at the "tail" of the cylindrical vessel. The flow is illustrated in two ways. Both figures demonstrate how the $z$-component of the rotation of the flow varies in the $xy$-plane. The first picture is produced with the *mesh* command in MATLAB. The second is a contrast adjusted grey-scale figure drawn with the aid of a program called Xfig. The profile should be "N-shaped", but due to the coarse mesh, the profile appears more like a sine wave, and it also becomes some pixels wider than the actual vessel. (It is of course somewhat unrealistic that a vessel ends abruptly as in these two examples, but to make the examples simple, the vessel was chosen to be a straight cylinder, and since the boundary condition is that the fluid must not leave the body, the abrupt cut-off is what resulted.)

If the vessel under investigation had been rotated 90 degrees, the "probe" could easily have been positioned at an other side of the square, i.e., parallel to the vessel, and the resulting tomographic image would be exactly the same as above. The "worst case" is therefore a vessel that subtends each side at an angle of 45 degrees. The second example, Figure 5, illustrates such a situation. The algorithm implemented has a tendency to gather the noise at the center of the body, parallel to the "long side", and in this second case, the amplitude of the noise is far greater than the actual "signal". However, since the parabolic flow profile generates an easily recognizable pattern, the vessel can still be detected. (The term *noise* is actually somewhat misleading, since all input data are exact. The reconstruction errors are due to discretization errors and to the fact that Beylkin's algorithm uses *pseudo*inverses of singular matrices.)
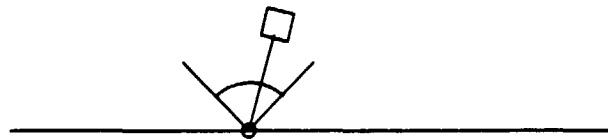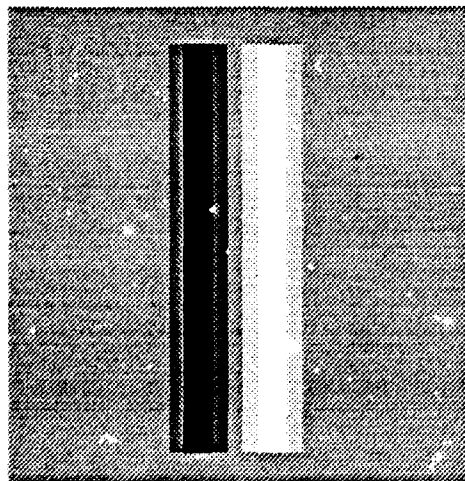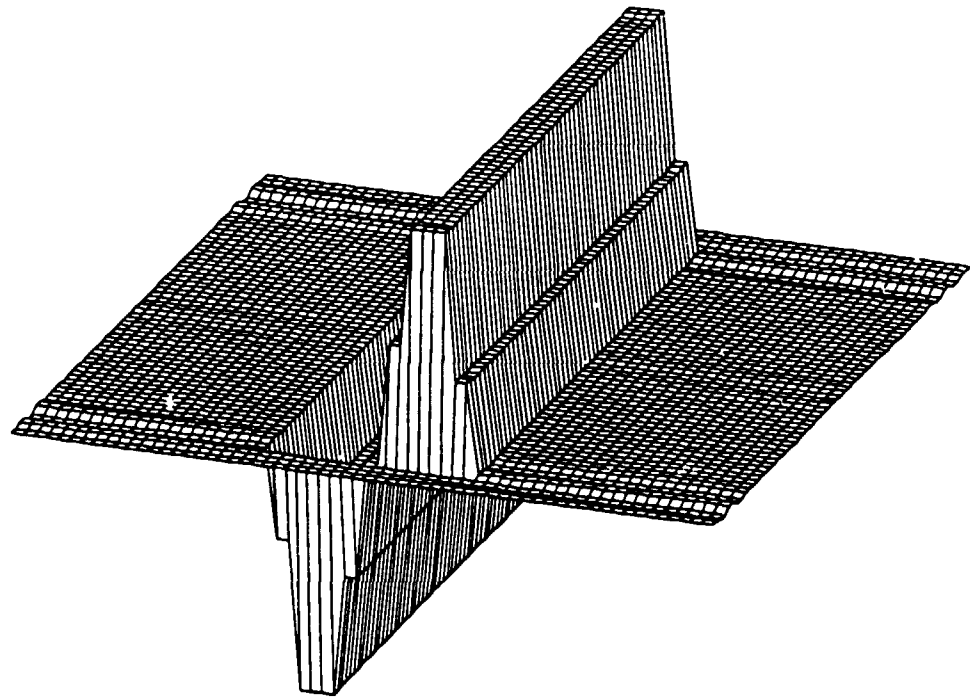
13

Figure 4: Computer simulated Doppler tomography of a parabolic flow approaching the observer. Both figures illustrate the "N-shaped" rotation field reconstructed by Beylkin's algorithm. Above is a MATLAB mesh, and below a grey-scale picture of the same flow. The Doppler probe is illustrated schematically in the lower figure. It is positioned at the side orthogonal to the vessel, and it is free to slide along this side. Its head can be turned freely in the span between 45° to the left and 45° to the right.
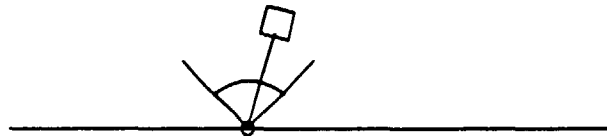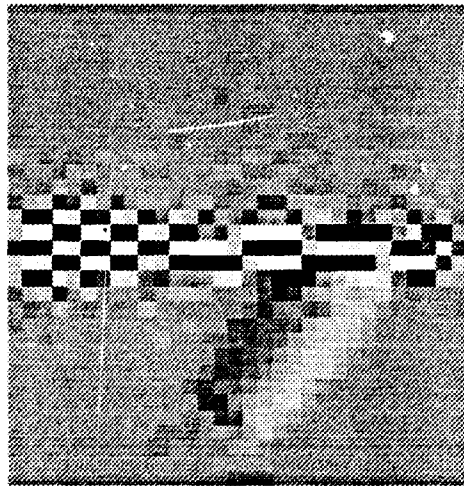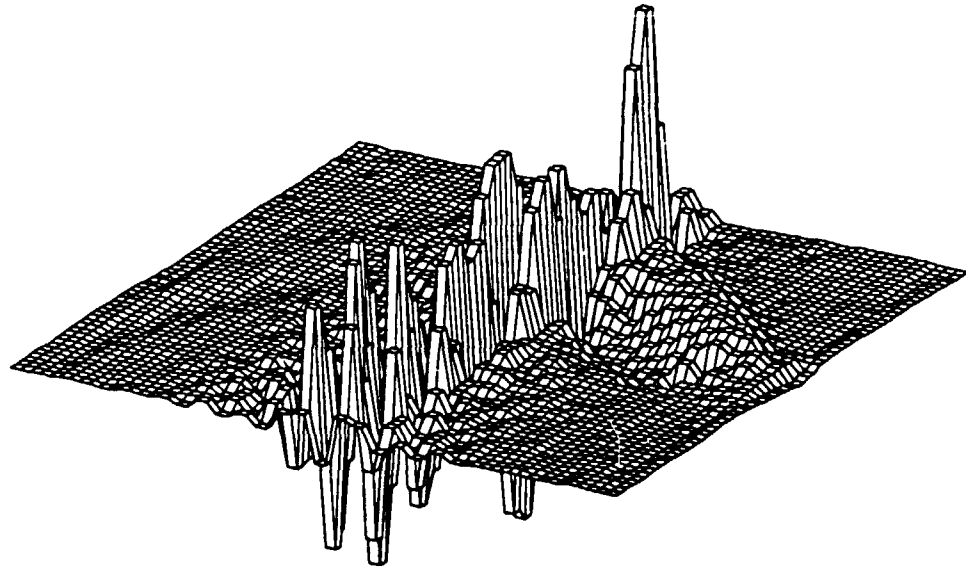
14

Figure 5: Computer simulated Doppler tomography of a parabolic flow. Both figures illustrate the rotation field reconstructed by Beylkin's algorithm. Above is a MATLAB mesh, and below a grey-scale picture. The horizontal string in the middle of the latter is "noise". The Doppler probe is illustrated schematically in the lower figure. It is positioned at the lower side parallel to the noise string, and it is free to slide along this side. Its head can be turned freely in the span between 45° to the left and 45° to the right. The vessel can be spotted in the lower right part of the figure, and it is oriented 45° oblique to the side along which the probe is moved.

When investigating flows in practical life, it would often be sufficient just to *spot* the vessel in a first scan. The probe can then usually be moved to become more aligned with the flow, thus giving a better resolution. Should it be possible to rotate the probe all the way around the body (like in X-ray computed tomography), an inversion scheme different from Beylkin's should probably be used, though. However, the aim of the computer simulations presented here was merely to get a conception of whether Doppler tomography might become practically useful.

## Future plans

The results so far seem promising, and the next step will be to measure on physical flows in a phantom provided by the group working with Doppler and Ultrasound imaging at the Department of Electrical Measurements.

The resolution of the mesh could be increased to at least $128 \times 128$ without creating unreasonable computing times. The simulations above have taken about one minute each on a Sun Sparc station, and the major part of that time is spent on the pseudoinversion of a matrix correlated to the experimental set up. This pseudo-inversion needs only to be performed once, and then the inverse Radon transform in essence is reduced to two fast Fourier transformations and a matrix multiplication.

Ideally, the differentiation should be performed already on the analogue Doppler signal, since convolving with a differentiation filter by necessity distorts the image, thus reducing the resolution. In the simulations presented above, the support of the differentiation filter was three pixels wide, which amounts to almost a tenth of the whole mesh, and that is far to much if the procedure should be of practical use.

## Acknowledgements

# References

[1] G. Beylkin. Discrete Radon Transform. *IEEE Transactions on Acoustics, Speech and Signal Processing,* 35(2), 1987.

[2] A. J. Chorin and J. E. Marsden. *A Mathematical Introduction to Fluid Mechanics.* Springer-Verlag, New York-Heidelberg-Berlin, 1979.

[3] S. R. Deans. *The Radon Transform and Some of Its Applications.* John Wiley & Sons, New York-Chichester-Brisbane-Toronto-Singapore, 1983.

[4] F. Natterer. *The Mathematics of Computerized Tomography.* John Wiley & Sons and B. G. Teubner, Stuttgart, Chichester-New York-Brisbane-Toronto-Singapore, 1986.